IEEE Access
Multidisciplinary | Rapid Review | Open Access Journal

Received May 19, 2021, accepted May 28, 2021, date of publication June 4, 2021, date of current version June 15, 2021.

Digital Object Identifier 10.1109/ACCESS.2021.3086628

Adaptive Flower Pollination Algorithm-Based Energy Efficient Routing Protocol for Multi-Robot Systems

KIRAN JOT SINGH[1], (Member, IEEE), ANAND NAYYAR[2,3], DIVNEET SINGH KAPOOR[1], (Member, IEEE), NITIN MITTAL[1], SHUBHAM MAHAJAN[4], (Member, IEEE), AMIT KANT PANDIT[4], (Senior Member, IEEE), AND MEHEDI MASUD[5], (Senior Member, IEEE)

[1]Embedded System and Robotics Research Group, Chandigarh University, Mohali 140413, India
[2]Graduate School, Duy Tan University, Da Nang 550000, Vietnam
[3]Faculty of Information Technology, Duy Tan University, Da Nang 550000, Vietnam
[4]School of Electronics and Communication, Shri Mata Vaishno Devi University, Katra 182320, India
[5]Department of Computer Science, College of Computers and Information Technology, Taif University, Taif 21944, Saudi Arabia

Corresponding authors: Kiran Jot Singh (kiranjot.693@gmail.com) and Anand Nayyar (anandnayyar@duytan.edu.vn)

This work was supported by the Taif University Researchers Supporting Project, Taif University, Taif, Saudi Arabia, under Grant TURSP-2020/10.

ABSTRACT The exploration and mapping of unknown environments, where the reliable exchange of data between the robots and the base station (BS) also plays a pivotal role, are some of the fundamental problems of mobile robotics. The maximum energy of a robot is utilized for navigation and communication. The communication between the robots and the BS is limited by the transmission range and the battery capacity. This situation inflicts constraints while designing an effective communication strategy for a multi-robot system (MRS). The biggest challenge lies in designing a unified framework for navigation and communication of the robots. The underlying notion is to utilize the minimum energy for communication (without limiting the range/efficiency of communication) to ensure that the maximum energy can be used for navigation (for larger area coverage). In this work, we present a communication strategy by using adaptive flower pollination optimization algorithm for MRS in conjunction with simultaneous localization and mapping (SLAM) technique for navigation and map making. The proposed strategy has been compared with multiple routing algorithms in terms of network life time and energy efficiency. The proposed strategy performs 4% better compared with harmony search algorithm (HSA) and approximately 10% better compared with distance aware residual energy-efficient stable election protocol (DARE-SEP) in terms of the total network lifetime when 50% of robots are alive. The performance drastically improves by 20% till the last robot is alive compared with HSA and approximately 26% compared with DARE-SEP. Hence, the energy saved during communication with the utilization of proposed strategy helps the robots explore more areas, which ultimately elevates the efficacy of the whole system.

INDEX TERMS Area exploration, multi-robot systems, optimization, robot communication, navigation, SLAM.

I. INTRODUCTION

''Unity is Strength'' is an insightful proverb that holds true for humans and robots in present times. Similar to humans, robots working together in proper coordination and cooperation perform better in various challenging situations. Multiple interacting dynamic objects or a group of robots functioning in an environment possessing some collective behavior is known as a multi-robot system (MRS) [1]. A team of several simple robots is always beneficial over a complex single robot because they offer a higher degree of reliability through resource repetitiveness and effectiveness by parallel task execution. The MRS also delivers better fault tolerance and flexibility because of dynamic reformation and coordination.

Recent progress in robotic research has allowed roboticists to use MRS for solving various real-world problems

The associate editor coordinating the review of this manuscript and approving it for publication was Zeyang Xia.

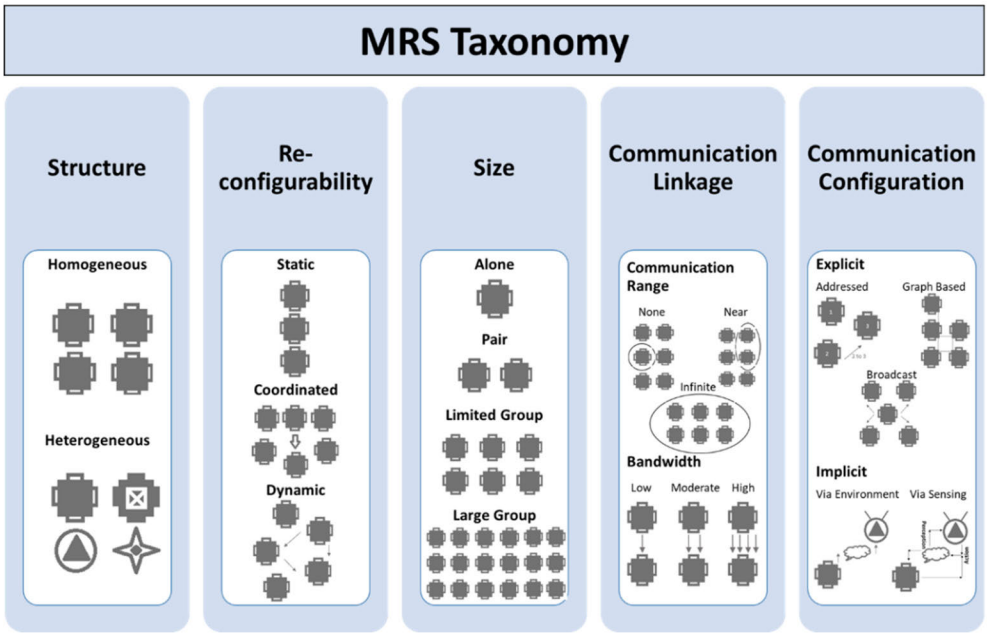

FIGURE 1. MRS taxonomy.

in various areas, such as agriculture, natural resource monitoring, emergency response and rescue, and maintenance of heavy machinery. Researchers worldwide have developed many projects of MRS catering to various applications [2]–[6]. Based on the research projects, the type of MRS applications can be further classified into unmanned ground vehicles, unmanned aerial vehicles (UAV), unmanned surface vehicles, and unmanned underwater vehicles (UUV). Various articles have been published in the area of MRS regarding survey analysis, review of research, frameworks, application domains, and taxonomies. Based on the literature available [7]–[14], MRS is classified into five groups (i.e., structure, re-configurability, size, communication linkage, and communication configuration), as depicted in Figure 1.

Structure or composition is defined as the type of hardware and software used for the robot team, and it can be homogeneous (a team of exactly the same robots) or heterogeneous (robots with different specifications). Re-configurability refers to the way of coordination among robots. This concept extensively depends on the application domain and the environment in which the robot team is operating. Re-configurability can be static (where no movement takes place), coordinated (where complete team is led by a single robot), or dynamic in which the decision process is autonomous for every individual robot. The size of the MRS is defined as the number of robots involved in a particular task. This mechanism is totally application-dependent. The team can be a pair of robots, a small team having 10–12 robots, or a large group (swarm) of robots.

Communication is a process in which data are transmitted and received between robots to accomplish the tasks. Further communication linkage or network refers to range/distance and bandwidth by which robots can connect to each other, and configuration/pattern defines the process of communication (i.e., explicit [indirect communication where information flow is through cloud] and implicit [direct connection between peer robots and BS] methods). The key factor for accomplishment of any task in an application is coordination among robots. Coordination can only be achieved by establishing communication between robots. Since the inception of MRS, constant developments have been observed in the communication strategies to enhance battery life and bandwidth utilization [15], [16]. The same can be used/modified for forest fire detection, habitat monitoring, and other surveillance applications [17].

The objectives of this work are as follows:

- Designing an enhanced MRS communication technique for the applications of field surveillance and search and rescue in military and urban domains
- Utilization of adaptive flower pollination optimization algorithm to minimize energy for communication purposes to maximize the energy being used for navigation
- Simulation-based experimental results of Adaptive Flower Pollination Algorithm (FPA) Energy Efficient Routing Protocol (AFPA-EERP) have been analyzed in terms of performance metrics, such as energy efficiency and network lifetime, performance at different energy levels, and effect of robot density, and are compared with different competitive algorithms.

A. ORGANIZATION OF PAPER

The paper is organized as follows: Section II highlights the real-world communication constraints for MRS. Section III elaborates the literature review. Section IV discusses related terminologies. Section V elaborates on the AFPA-EERP

Protocol for communication. Section VI elaborates the simulation results. Section VII concludes the paper with future scope.

II. REAL WORLD COMMUNICATION CONSTRAINTS FOR MRS

Effective communication among robots is one of the biggest and vital challenge in MRS. The quality of communication degrades in the exploration domain because of distance between peer robots or base station (BS), obstacles, and many other geographical factors. Wireless network with large bandwidth provides satisfactory communication [18]. However, this notion is not true because real world conditions and network must be intelligently planned to overcome overloading and conservation of energy because of large number of robots.

Communication support is a costly in terms of energy consumption because more payload will rapidly drain the battery. Some potential parameters that must be considered while transmitting data from a robot are individual state, task data, and environmental state. Individual state represents battery level and robot identification, task data refer to task specific information provided by sensors, and environmental state characterizes hazardous variations in the environment, which can constrain reliable communication between robots [19]. The communication standards, such as Wireless Fidelity, Radio frequency, and Infra-Red (IR) to be deployed for MRS, must be considered depending on certain factors, such as geography, distance, and line of sight, for a particular application.

The type of communication configuration, which can be implicit or explicit, is also important for efficient information sharing in MRS for geographically reliant applications. Moreover, the type of communication strategy used plays a crucial role in dissemination/reception of information to/from robots in a timely manner to reduce conflicts and delay. Hence, the cost of communication is a function of certain parameters, transmission time, collision with other robots, and energy consumed to fix communication range and strategy [20], [21]. In summary, real world communication constraints must be considered before deciding communication technology, bandwidth allocation, and communication strategy.

In this section, the communication constraints in the example scenarios of field surveillance, search and rescue, and monitoring systems have been discussed. The MRS is deployed in these setups to achieve higher efficiency, economical deployment, and redundancy, which is beyond the scope of single robot systems [22].

A. EXAMPLE SCENARIO 1: MRS IN THE STABLE LAYOUT DOMAIN

This type of scenario arises in certain applications, such as forest fire detection, habitat monitoring, aerial robotics, and other monitoring systems. Robots maintain a specific type of formation in these applications (Figure 2) and are controlled by BS. Robots establish recurrent connectivity, which refers to connectivity activated due to the occurrence of an event or timeout; thus, the bandwidth required is low. Peer to peer connection is established between robots in the dynamic environment, where only location coordinates are shared to maintain formation. The BS has to plan the communication path (robot–robot and robot–BS) in an optimized manner to reduce transmission time and battery consumption for maximum network lifetime.

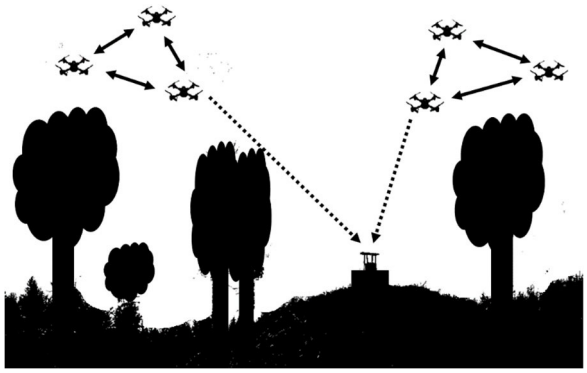

FIGURE 2. MRS in the stable layout domain (aerial robotics).

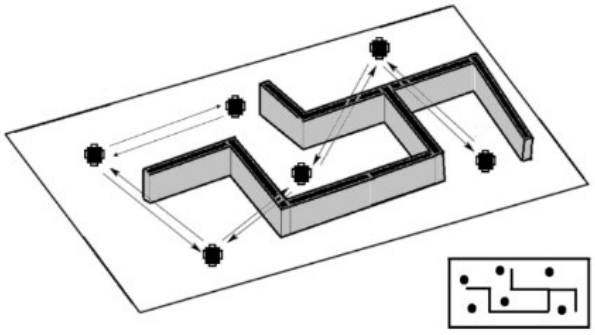

FIGURE 3. MRS in the collaborative layout domain (map building).

B. EXAMPLE SCENARIO 2: MRS IN THE COLLABORATIVE LAYOUT DOMAIN

This scenario is common to certain applications, such as search and rescue operations, underwater exploration, map building for houses, factories, and other unknown environments. Given that geographical topology is not/partially known to MRS, robot location and path cannot be planned in advance (Figure 3). In this case, robots continually share information with peer robots and BS. The delay in information reception in these applications result in failure of the system. During search and rescue operations, robots must send real time images/data to BS to ensure that effective decisions can be timely carried out. Hence, a higher bandwidth is required for efficient data transfer between robots and BS. Robots have to communicate through various obstacles/scatterers because the terrain is unknown; hence, an omnidirectional antenna with higher communication ranges are necessary for robots. The key factors that limit

the system performance are continuous connectivity, higher bandwidth, and network congestion.

III. LITERATURE REVIEW

The research in the routing protocols based on clusters mainly concentrates on three objectives: dropping delay, energy saving, and improving accuracy. This notion means that a routing protocol offers a good performance for MRS data aggregation, if it can collect the maximum number of packets with minimum energy consumption and delay. However, these objectives are declared and enhanced in accordance with the consumer/application requirements. Akyildiz *et al.* [23] proposed that a protocol with the least delay and best accuracy is suited for real time applications, even if it does not enhance energy efficacy. The potential correlations between energy, delay, and the number of collected data samples should also be taken care by routing protocols [24]–[26]. For example, collecting a greater number of packets increases energy consumption and delay, especially when the data sources are randomly scattered in the network. Dutta *et al.* [27] proposed a scalable peer-to-peer radio communication framework for MRS. The essence of their framework is to ensure that the message reaches the destination in minimum number of hops. Hu *et al.* discussed that [28] utilizing direct communication instead of multi-hop to reduce the delay increases consumption of energy, whereas data collection delay is increased by using multi-hop routing. Accordingly, the issues of energy conservation, reducing delay and/or increasing the unit of collected data items, need to be addressed to design data aggregation routing protocols and enhance their performance in MRS.

Many studies have discussed [29]–[34] about distributed data aggregation protocol supporting multi-hop data transmission for multi-robot communication. They also discussed about the energy consumption needs to be reduced because a robot has limited power. Energy squandering hinges on the number of transmissions, dissemination stretch, and data aggregation computation overhead. For this reason, data aggregation protocols should minimize the network traffic and path leap count. Data aggregation routing delay should be minimized for data freshness. Specifically, routing delay may change the meaning and impact of collected data on further processing at BS. Data aggregation delay depends on network congestion (network traffic), transmission distance, and communication delays. Increasing the count of captured data samples enhances data collection robustness. The data consumer can make precise decisions on the collected data if a greater number of data samples are collected. Data accuracy depends on the routing algorithm's effectiveness to report data samples to the BS.

The above discussion shows that one single common default protocol will not suit each application, and an appropriate parameter setting is necessary for stabilizing the energy dissipation with other competing metrics, such as delay and data accuracy. Therefore, a method that can efficiently and inevitably choose a suitable protocol parameter is always sought by roboticists. The network layer in MRS routing protocol stack accomplishes data routing and self-configuration of the network. This mechanism finds the finest route to ensure that the energy consumption of the mobile robots is minimized. The method is also accountable for updating the network topology if any link failure occurs.

Network layer energy-aware routing algorithms can be classified into various categories, consolidated in Table 1 [35], [36], [45]–[54], [37]–[44]. Various optimization techniques, such as Genetic Algorithm [55], Particle Swarm Optimization (PSO) [56], Ant Colony Optimization (ACO) [33], [57], and Harmony Search Algorithm (HSA) [58], have also been used in this regard. These techniques utilize distinctive parameters in wellness capacity to achieve their goals.

A robot with low energy can become a cluster head robot (CHR), considering that the point selection of CHR is probabilistic, as revealed by literature. Hence, CHR selection in a deterministic way must be considered along with the residual energy of robots. Other factors can also be considered to balance the load of robots, such as distance from the BS and the other robots from CHR. Therefore, the elementary requirement for energy efficient routing protocol for communication is proper selection of CHR in appropriately formed cluster. CHRs are usually assumed to have long communication range and can directly connect to the BS. However, this assumption is unrealistic because BS is often times not reachable due to the losses in signal propagation.

One of the solutions to handle this problem is to deploy multi-hop communication between the robots and the BS. The literature reveals that many evolutionary algorithms have done better than deterministic methods in many problems related with CHR selection in MRS. Appropriate selection of evolutionary algorithms alongside proper fitness function can proficiently balance the depletion of energy depletion in robots and hence uplift the lifetime of network. FPA is a newly developed heuristic approach that imitates the pollination procedure of flowers [59], [60] and has been effectively useful for problems of forest fire detection [61] and antenna design [62]. In this work, the potential of FPA has been exploited for resolving the problem of load balancing in clusters to proficiently balance the consumption of energy in robots and maximize the period of stability for the communication network.

IV. FLOWER POLLINATION ALGORITHM

FPA takes its inspiration from the natural pollination mechanism of flowering plants [60]. Each flower in FPA stands for a viable solution, and the objective function value is considered to be its fitness value. Two separate pollination phases are used to mimic the pollination process: Global and local pollination phases are used for each flower to mimic the pollination process with a switch probability p_s, as shown in Algorithm 1. The detailed process of FPA is as follows.

Global pollination phase: Initially, a random number rand is created for each individual. If rand $< p_s$, then the global pollination phase should be carried out. Every flower updates

TABLE 1. Network layer energy aware routing classifications in MRS [34]–[51].

S. no.	Classification	Type	Features
1	Mode of function based	Proactive	• In-advance route determination • Routing table used for storing information about routes • Every robot maintains its own routing table
2		Reactive	• Route is not computed until it is required. • Routes is computed on the basis of the demand. • No overhead on robot, as no need to maintain routing table by the robot
3		Hybrid	• Combination/mixture of reactive and proactive protocols
4	Participation style based	Direct	• Information is sent by all robots to BS. • Heterogeneous functionality
5		Flat	• Homogenous functionality • Flat network structure • Every robot executes sending and sensing tasks
6		Clustering	• Robots are categorized in different clusters. • Cluster head robot (CHR) is chosen form every cluster. • Member robots sent data to CHR, and CHR further sends data to BS.
7	Network structure-based	Data centric	• Query-based protocols. • Data diffusion conducted by robots by using naming schemes. • ACQUIRE and SPIN
8		Hierarchical	• Energy efficient routing • Low energy robots send data to high energy robots, which further send data to BS. • Examples include LEACH-C, PEGASIS, TEEN, and APTEEN
9		Location based	• Routing is determined on the basis of the location of robots. • Received signal strength or global positioning system (GPS) is used to measure distance between robots. • Examples include DREAM, GEAR, IGF, OGF and HGR
10		QoS aware	• Focuses on QoS parameters (e.g., delay, latency, reliability, and bandwidth) • Maintaining balance between QoS parameters and consumption of energy. • Examples include SAR, SPEED, MMSPEED, and MGR

its position in the global pollination process according to the following equation [60]:

$$X_i^{t+1} = X_i^t + \gamma L(\lambda)\left(X_{best}^t - X_i^t\right), \tag{1}$$

where X_i^t and X_i^{t+1} are the previous and updated positions of the i^{th} flower, respectively; X_{best}^t is the best flower that has the best fitness value at current iteration t, and γ is used as a scaling factor to control the step size of global pollination. Lévy flight L is used as the strength of pollination in the basic FPA, and the step size (λ) obeys the Lévy distribution:

$$L \sim \frac{\lambda\Gamma(\lambda)\sin(\pi\lambda/2)}{\pi}\frac{1}{s^{1+\lambda}}, \quad (s \gg s_0 > 0), \tag{2}$$

where $\Gamma(\lambda)$ is the gamma function.

Local pollination phase: The local pollination process is selected for the case rand $> p_s$. Flower X_i^t attains its updated position X_i^{t+1},, employing the difference between its previous position and the position of two adjacent flowers, namely, X_p^t and X_q^t. This step is considered to be a local random walk [60] and is expressed as follows:

$$X_i^{t+1} = X_i^t + r(X_p^t - X_q^t), \tag{3}$$

where r is a uniformly distributed random number [0, 1].

The new individuals change their positions after completion of the pollination phases by comparing their fitness values. If the fitness of X_i^{t+1} is better than that of X_i^t, X_i^{t+1} will replace the new position of its flower. Otherwise, the flower stays at the X_i^t position. The FPA has gained attention because of its linear nature and its effectiveness in the recent past and large number of developments in its basic form as has been done since its inception. In this work, an enhanced version of

FPA called adaptive FPA (A-FPA) is used to resolve the load balancing problem in the MRS.

Algorithm 1 1: Pseudocode of FPA

Start:

Initialize a population of $\varkappa$ *random flowers*
Define switch probability, $\boldsymbol{p}$
Define objective function
Identify current best solution $\boldsymbol{X^t_{best}}$
while $\boldsymbol{t} < max(\boldsymbol{t})$
  for $i = 1$:
    if $\mathfrak{X} < \boldsymbol{p}$
    perform Global Pollination:
    $\boldsymbol{X^{t+1}} = \boldsymbol{X^t_{\varkappa}} + \boldsymbol{\gamma L}(\lambda)(\boldsymbol{X^t_{best}} - \boldsymbol{X^t_{\varkappa}})$
    else
    perform Local Pollination:
    $\boldsymbol{X^{t+1}_{\varkappa}} = \boldsymbol{X^t_{\varkappa}} + \boldsymbol{r}(\boldsymbol{X^t_p} - \boldsymbol{X^t_q})$
    end if
    evaluate $\boldsymbol{X^{t+1}_{\varkappa}}$
    if $\boldsymbol{X^{t+1}_{\varkappa}}$ *is better than* $\boldsymbol{X^t_{\varkappa}}$, *update position*
    end if
  end for
  Find the Current best
end while
Update Final best

End

V. PROPOSED AFPA-EERP PROTOCOL FOR COMMUNICATION

A. PROBLEM FORMULATION

The problem addressed in this correspondence is effective communication for the application of unknown open environment exploration for the generation of maps and/or search and rescue missions. An initially unfamiliar, circumscribed, continuous 2D area $\mathrm{U} \subset \mathbb{R}^2$ is considered, where $\mathbb{R}^2$ signifies that the locations on U represented by x and y refer to the latitude and longitude coordinates of the GPS, respectively. A team of M mobile robots $X = (X_1, X_2, \ldots, X_M)$ will send data to the principal control center called the BS located at a fixed location outside the bounds of U. Each robot integrates various types of sensors, such as ultrasonic [63], LIDAR [64], thermal [65], image [66], and GPS [67], to perceive the environment and transceivers (Texas CC1120 [68], Microchip RN2483 [69], Semtech SX1272 [70], etc.) for long range data transmission and reception. Every robot is capable of exchanging data with the BS and other robots over an ad-hoc wireless network governed by the proposed algorithm (discussed in the subsequent section). The BS plans the path and pose for each robot through simultaneous localization and mapping algorithm (SLAM) [71], [72] to safeguard the autonomy of robot. The progression of time is considered in discrete steps (i.e., $t \in \{1, 2, \ldots, \mathrm{T}\}$, where last time step of the mission is denoted by T). The speed, position, direction and transmission range of the robots are represented by a pose function of the robot, given as follows:

$$\psi_m^t = f(\mathrm{U}_m(x, y), \vartheta_m, \theta_m, \mathcal{L}_m), \tag{4}$$

where $\mathrm{U}_m(x, y)$ is the position, ϑ_m is the speed, θ_m is direction, and $\mathcal{L}_m$ is the transmission range of robot X_m at time t.

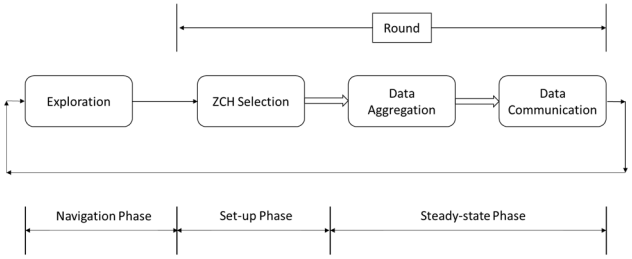

FIGURE 4. Process of exploration and communication

B. SYSTEM MODEL

In this work, an improved FPA called AFPA-EERP has been proposed in this work. This method seeks to achieve improved performance by enhancing the basic FPA. The various tasks performed by robots are sensing, computing, transmitting, and receiving. Few robots are zone cluster head (ZCH) or leaders; they collect and process the data and then forward it to BS. The task of robots (i.e., zone member robots [ZMR]) other than ZCH is to sense the surroundings and send the data to the ZCH of their respective zone.

The complete process of exploration and communication is performed in three phases. The first phase is the navigation phase, in which robots sense the environment till particular time interval $t = t_o$ decided by base station and stop moving till the next instruction by BS. The second phase is set-up phase, wherein ZCH selection is performed. The third phrase is the steady-state phase, which is responsible for routing. Once the steady-state phase is over, the BS again initiates the navigation phase. The complete process of exploration and communication is shown in Figure 4.

C. EXPLORATION

According to the system paradigm described above, the exploration of the unknown territory is processed as follows: the area to be explored is divided into $g \times h$ matrix, where g and h are whole numbers. Every element of the matrix is called zone, which is given as follows:

$$\mathrm{U} = \cup_{g,h} z(g, h). \tag{5}$$

Considering $g = h = 3$, U is divided into 3×3 matrix (i.e., nine zones). A number of robots (ten in our case) are placed at the boundaries of the peripheral zones of U. At a particular time t, the deployment of robots is given as follows:

$$\mathfrak{D}^t = (\psi_1^t, \psi_2^t, \psi_3^t, \ldots . \psi_M^t). \tag{6}$$

The SLAM algorithm is used to cater to the challenge of map building because of its high convergence and ability to handle uncertainty efficiently [73], [74]. A graph-based

SLAM approach is followed to represent the map in terms of finite vector $\mathscr{b}$ by m^{th} robot to record the corresponding observations $e_m^{\mathscr{t}}$ from the LIDAR sensors. Odometry measurements $q_m^{\mathscr{t}}$ are executed at time steps t to register a new pose function $\psi_m^{\mathscr{t}+1}$ of the robot, which is given as follows:

$$q_m^{\mathscr{t}} = \left(\frac{\psi_m^{\mathscr{t}}}{\psi_m^{\mathscr{t}+1}}\right), \tag{7}$$

where $\psi_m^{\mathscr{t}}$ and $\psi_m^{\mathscr{t}+1}$ refers to before and after the movement poses of the m^{th} robot. At time $\mathscr{t}$, the appraised joint posterior over the map in probabilistic form is given as follows [72]:

$$\wp(\psi m^{1:\mathscr{t}}\, \mathscr{b} | e_m^{0:\mathscr{t}}, q_m^{0\mathscr{t}-1}, \psi_m^0). \tag{8}$$

The integration of sensor data to find the maximum likelihood is re-appraised for the whole map in each iteration to store the overall data, as expressed below:

$$\begin{aligned}\wp(\psi_m^{\mathscr{t}}, \mathscr{b} | e_m^{0:\mathscr{t}}, q_m^{\mathscr{t}}, \psi_m^0) \\ = \int\int\ldots\int \wp(\psi m^{1:\mathscr{t}}, \mathscr{b} | e_m^{0:\mathscr{t}}, q_m^{0:\mathscr{t}-1}, \psi_m^0) \\ \times d\psi_m^1 d\psi_m^2 \ldots d\psi_m^{\mathscr{t}-1}.\end{aligned} \tag{9}$$

Map construction in graph-based SLAM is a two-step procedure. The first step named as front-end is to describe and integrate constraints and is highly sensor-dependent; the second step named as back-end is abstract depiction of data and is sensor agnostic [72], [75]. Thus, the objective function to find the configuration of robots is given as follows:

$$\mathfrak{f}\left(\psi_m^1, \ldots., \psi_m^{\mathscr{t}}\right) = \sum\nolimits_{u,v} e_{u,v}^T \mho_{u,v} e_{u,v}, \tag{10}$$

where $e_{u,v}$ is the difference of the appraised and observed poses, and $\mho_{u,v}$ represents the information matrix.

At a particular time interval $\mathscr{t} = \mathscr{t}_o$ decided by base station, the robots stop moving and transmit their data to their respective ZCH, which further transmits the data to BS. The SLAM algorithm is computed at the BS to update the uncertainty grid [76], which in turn calculates the updated pose function $\psi_m^{\mathscr{t}}$, for all robots. This information is transmitted back to ZCH, which forwards the same to its ZMR for further navigation. All robots will be made to converge toward the central zone (i.e., $g = h = 2$), as shown in Figure 5. At the central zone, ten robots with maximum energy will be selected by the BS from all of the robots, and the same process is repeated again for the central zone.

D. RADIO ENERGY DISSIPATION MODEL FOR COMMUNICATION

Given that robots have limited energy, the power consumption is a crucial aspect for scheming communication protocol because energy is consumed by robots for sensing, navigation, data processing, and wireless communication. During communication, the network consumes energy from both sides (sender and receiver) as per the wireless energy consumption model depicted in Figure 6. This model involves two parts that reflect transmission and reception, as depicted in Equations 12 and 14, respectively [40]. Robots consume energy E_{TX} to power-up the transmitter circuit and E_{amp} to actuate the transmitter amplifier. Meanwhile, the wireless receiver consumes E_{RX} amount of energy to activate/actuate the receiver circuit. In the underlying wireless communication, the energy consumption also depends on the message length l. Thus, the transmission cost for sending the message, which is l-bit long and has the transmitter–receiver distance d, is calculated as follows:

$$E_{TX} = \begin{cases} lE_{elec} + lE_{friis\_amp}d^2, & if\ d < d_0 \\ lE_{elec} + lE_{two\_ray\_amp}d^4, & if\ d \geq d_0 \end{cases}, \tag{11}$$

where d_0 is the crossover distance and is given by:

$$d_0 = \sqrt{E_{friis\_amp}/E_{two\_ray\_amp}}, \tag{12}$$

where E_{elec} signifies the energy consumed per bit for transmission, E_{friis_amp} represents the energy consumed, and $E_{two\_ray\_amp}$ denotes the energy consumed in the two-ray ground propagation by the radio. The reception cost for the l-bit data message received is given as follows:

$$E_{RX} = lE_{elec}. \tag{13}$$

E. WORKING

The protocol process is bifurcated into rounds consisting of set-up and steady-state phases, as illustrated in Figure 7. The optimum ZCH selection is performed in the set-up phase, and the optimum route is established in the steady state phase by using AFPA-EERP. The ZCHs are selected by the BS from the alive robots that have residual energy more than a threshold level by using AFPA-EERP, which is basically the average energy of all robots that are active, in the set-up phase. First, the BS makes announcement of a short communication to obtain the identifications, energy levels, and locations of every robot present in the particular zone. Based on the received data by the robots, the BS uses AFPA-EERP to elect the ZCH per zone on the basis of minimization of fitness function given by equation 14.

The whole process is to minimize the fitness function and ZCH selection, which is formulated as Pseudocode 1. When ZCHs are elected, and their associate members (i.e., ZMRs) are determined, a communication broadcast is launched by the BS to inform robots in various zones about their respective ZCH and ZMRs in association. A time division multiple access (TDMA) schedule is generated by the elected ZCH to assign time slot to ZMRs and further notify with schedule through broadcasting in their zone. The schedule of TDMA is used to avoid intra-group interference and provides a facilitation to every ZMR for shutting down their radios when not in operation for energy conservation. To reduce the inter-zone interference, a distinctive code division multiple access (CDMA) code is chosen by each ZCH, and notification is sent to all associated ZMRs present within the zone to use this code to send their information.

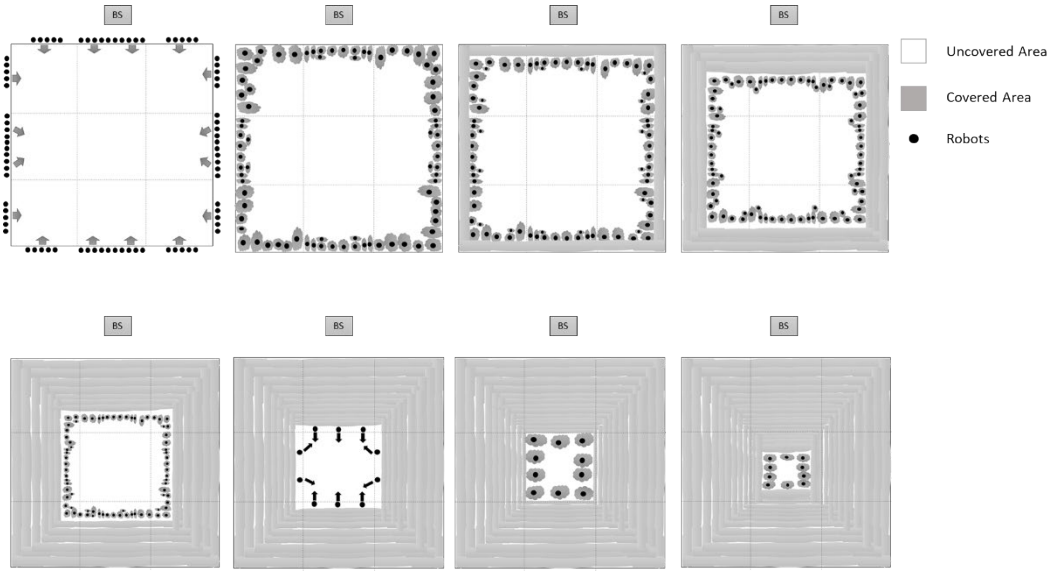

FIGURE 5. Robot navigation in 3 × 3 field.

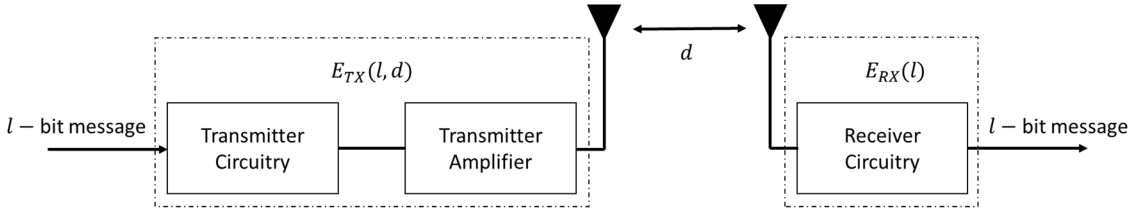

FIGURE 6. Radio energy dissipation model.

1) FITNESS EVALUATION

Let us consider a network of M robots deployed in area $\mho$. Let $X = (X_1, X_2, \ldots, X_M)$ denote the population vector of a robots with M robots, where the position of the m^{th} robot in the j^{th} zone is $X_m(j) = \{0, 1\}$. ZMRs and ZCHs are represented by values zero and one, respectively. The Np solutions (size of population) is randomly initialized in terms of ones and zeros. One ZCH is selected per zone. The robots are deployed into Z zones, where $Z = z(g, h)$, and g and h are whole numbers. The fitness function for ZCH selection is defined as follows:

$$f_{\text{obj\_ZCH}} = (f_1 + f_2)/2, \tag{14}$$

subject to $\sum_{i=1}^{2} w_i = 1$, where w_i is.5 to provide equal contribution to both fitness functions.

Reduction of standard deviation of the remaining/residual energy of each robot is crucial to accomplish the better stability period. The standard deviation (σ_{RE}) aids in measuring the quality of even dissemination of the load between robots per Z, which is given as follows:

$$f_1 = \sigma_{RE} = \sqrt{\frac{1}{M}\sum_{m=1}^{M}\{\mu_{RE} - E(X_m)\}^2}, \tag{15}$$

where $\mu_{RE} = \frac{1}{M}\sum_{m=1}^{M} E(X_m)$, and $E(X_m)$ is the remaining/residual energy of the mth robot.

The second objective concerns with aggregation of the residual energy level $E(X_m)$ and average distance value A_D for the selection of ZCH.

$$f_2 = ZH_{EV}(m) = 0.5E(X_m) + 0.5(1/A_D(m)), \tag{16}$$

where A_D is average distance of a robot from all the other robots in the same zone, as provided in Equation (17). The chance of a robot to become ZCH is elevated with its lesser average distance A_D.

$$A_D(m) = \frac{1}{M-1}\sum_{m=1}^{N} d(m, n), \quad m \neq n, \tag{17}$$

where N is the total number of robots in a zone, and $d(m, n)$ is the distance of the mth robot from the nth robot in its zone, as follows:

$$d(m, n) = \sqrt{(m_x - n_x)^2 + (m_y - n_y)^2}. \tag{18}$$

F. ALGORITHM

In this work, an improved FPA called adaptive FPA is used to attain advance performance by enhancing the basic FPA's diversification (or exploration) and intensification (or exploitation) capabilities [77]–[79]. Diversification has been enhanced by using the Elite Opposition-based Learning (OBL) (EOBL) strategy [80]. Global pollination phase has been improved by Cauchy-based step size that helps in effectively exploring the search space [81]. Intensification has

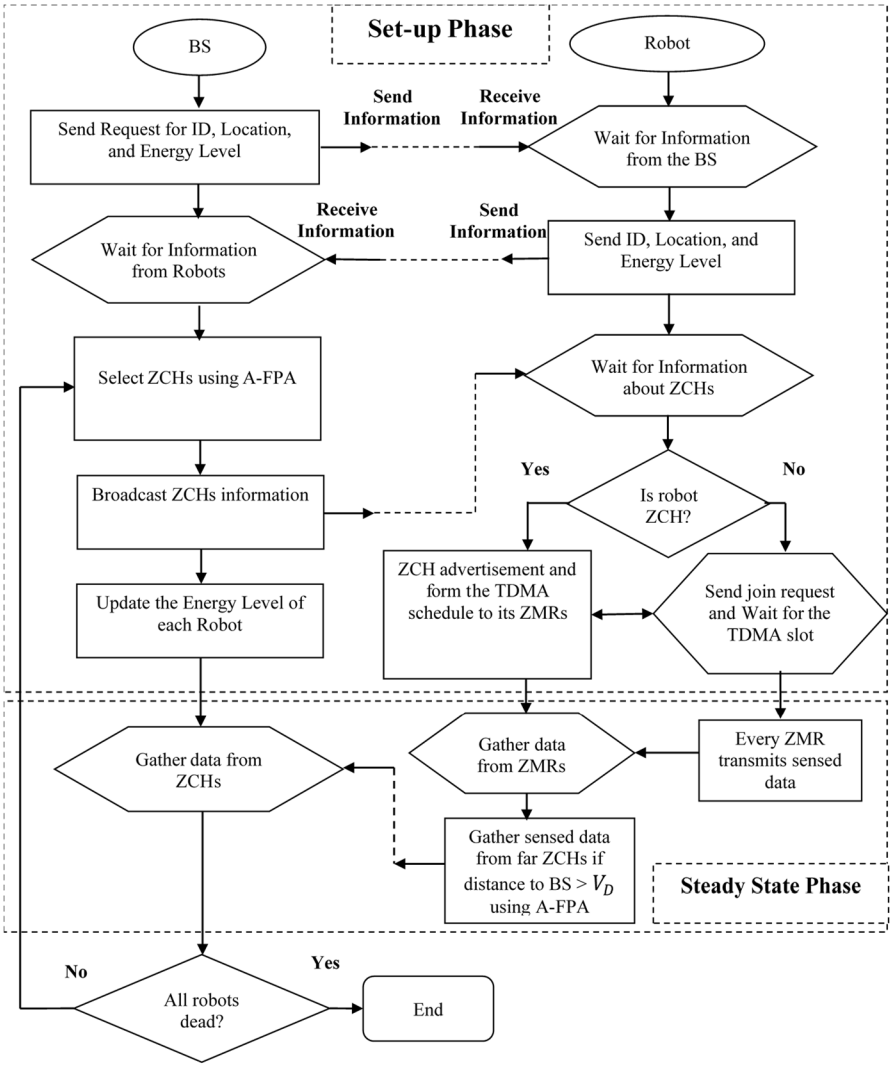

FIGURE 7. Working of proposed AFPA-EERP protocol.

been improved by the Local Neighborhood Search (LNS) determined by the best solution obtained in a small neighborhood of the present solution [82]. The dynamic switch probability (p_t) [83] is used to achieve a balance between diversification and intensification. The catfish-effect mechanism [84] is presented to circumvent premature convergence. The major modifications are as follows::

1) STRATEGY FOR EOBL

In conventional FPA, the optimal global solution is difficult to achieve once the algorithm falls to the local optimal. Therefore, the current solution space approximation must be directed to the global optimal solution space. The EOBL approach has been employed to enhance the global search capabilities of the FPA [80].

Before introducing the EOBL, we will first explain OBL. The core principle of OBL is that it creates the opposition solution of the existing solution, simultaneously compares the current solution and the opposition solution, and selects the better output to move to the next iteration. We assume that $x = (x_1, x_2, x_3, \ldots, x_D)$ is a solution in the population (D is the dimension of search space; $x_j \in [a_j, b_j]$, $j = 1, 2, \ldots, D$), and its opposition solution is expressed as $\tilde{x} = (\tilde{x}_1, x_2, \tilde{x}_3, \ldots, \tilde{x}_D)$, where

$$\tilde{x}_j = a_j + b_j - x_j. \tag{19}$$

The OBL opposition solution created could not be promising to find the optimal global solution other than the current search space; hence, we will use the EOBL strategy [80]. EOBL is an intelligence computing technique. This work assumes that $X_e = (x_{e,1}, x_{e,2}, x_{e,3}, \ldots, x_{e,D})$ is the elite (optimal) solution in the population. With regard to individual X_i, the elite opposition solution $\tilde{X}_i$ is given by

$$\tilde{x}_{i,j} = \eta * (da_j + db_j) - x_{e,j}, \tag{20}$$

where $i = 1, 2, \ldots, NP$; $j = 1, 2, \ldots, D$; NP is the population size, $\eta \in U(0, 1)$ is a generalized coefficient, and $[da_j, db_j]$ is the dynamic boundary of the jth dimensional

search space and is represented by:

$$da_j = \min\left(x_{i,j}\right), \quad db_j = \max\left(x_{i,j}\right). \tag{21}$$

To maintain the search experience, the dynamic boundary is used instead of a fixed boundary to render the opposite solution located in the narrowing search space. If $\tilde{x}_{i,j}$ jumps from $[da_j, db_j]$ because of the dynamic boundary operator, then the following tactic is employed to reset $\tilde{x}_{i,j}$:

$$\tilde{x}_{i,j} = rand(da_j, db_j). \tag{22}$$

In EOBL, the opposition solutions are created according to the elite solution. This approach uses the elite solution characteristics to provide more valuable search information that will help in improving the diversity of the population and the FPA's global diversification trend.

2) CAUCHY DISTRIBUTION-BASED GLOBAL POLLINATION PHASE

Each flower in the global pollination phase of the basic FPA updates its position according to:

$$X_i^{t+1} = X_i^t + \gamma L(\lambda)(X_{best}^t - X_i^t), \tag{23}$$

where X_i^t and X_i^{t+1} are the previous and current positions of the i^{th} flower, respectively; X_{best}^t is the flower with best fitness at iteration t; and γ is the scaling parameter to control the global pollination phase step size. The function of Lévy flight parameter L is to strengthen the pollination in the conventional FPA. The step size (λ) follows the Lévy distribution:

$$L \sim \frac{\lambda\Gamma(\lambda)\sin(\pi\lambda/2)}{\pi}\frac{1}{s^{1+\lambda}}, \quad (s \gg s_0 > 0), \tag{24}$$

where $\Gamma(\lambda)$ is the gamma function.

In the proposed A-FPA, the heavy tailed and highly directed Cauchy-based step size is utilized instead of Lévy flights used in conventional FPA [81]. This Cauchy-based step size is better at exploring the search space due to its heavy tailed distribution and is given by

$$dis = \frac{1}{2} + \frac{1}{\pi}\arctan\left(\frac{\delta}{g}\right). \tag{25}$$

The Cauchy density function is represented as follows:

$$f_{Cauchy(0,g)}\,(dis) = \frac{1}{\pi}\frac{g}{g^2 + x^2}, \tag{26}$$

where g is a scaling parameter with a value equal to one, δ is the Cauchy random operator, and dis is a uniform random number. The position updating equation for the global pollination phase by using the Cauchy distribution function is given by:

$$X_i^{t+1} = X_i^t + C(\delta)(X_{best}^t - X_i^t). \tag{27}$$

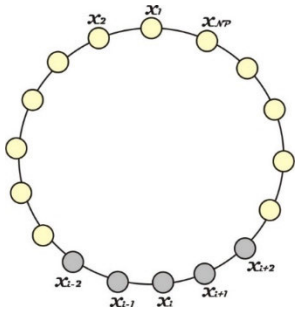

FIGURE 8. Neighborhood ring topology of radius 2.

3) LNS

FPA uses the best current and random solutions to expand local search in the local pollination phase. The LNS model [82] is used to strengthen the local search capability of the basic FPA.

The key idea is to use the current best solution in a small neighborhood of the current solution to improve the current solution. The knowledge of an individual's neighborhood is utilized for updating the position of the individual.

We suppose that the population is a vector in the current population (i.e., $X = (X_1, X_2, X_3, \ldots, X_{NP})$, X_i ($i \in [1, NP]$). Here, each vector's indices are random to preserve each neighborhood's diversity. Now, we define the radius r neighborhood (r is a nonzero integer, and $2r + 1 < NP$) for each X_i. The neighborhood of X_i consists of $X_{i-k}, \ldots, X_i, \ldots, X_{i+k}$. Figure 8 shows the notion of the local neighborhood model in that the vectors can be organized into a ring topology according to their indices. The LNS model is defined as

$$L_i = X_i + m * \left(X_{n\_opt} - X_i\right) + n * (X_p - X_q), \tag{28}$$

where $p, q \in [i - r, i + r]$ ($p \neq q \neq i$), and m and n are the scaling factors, where $m, n \in$ rand (), and X_{n_opt} is the best solution in the X_i neighborhood. The enhanced version of FPA updates the best solution according to (13), and the modified solution performs the local pollination step as follows:

$$X_i^{t+1} = L_i^t + r * (X_k^t - X_m^t), \tag{29}$$

where L_i is the best solution obtained using LNS, and X_k^t and X_m^t are the random solutions of the k^{th} and m^{th} flower, where $k \neq m$, and r is a randomly generated scaling factor.

4) DYNAMIC SWITCH PROBABILITY

In adaptive FPA, instead of using a fixed switch, an adaptive switch (p_t) has been designed to balance the diversification and intensification tendency during the search process [83]. The search agents can use this approach to update their position in accordance with the present fitness value variation,

as follows:

$$X_i^{t+1} = \begin{cases} X_i^t + C(\delta)(X_{best}^t - X_i^t), & rand > p_t \\ X_i^t + m * \left(X_{n\_opt}^t - X_i^t\right) & \\ +n * \left(X_p^t - X_q^t\right) + r * \left(X_k^t - X_m^t\right), & rand \leq p_t \end{cases}, \tag{30}$$

where p_t is evaluated in the previous iteration. The exploitation must be preferred with a higher probability compared with the exploration mode to accelerate the optimizer convergence. Thus, the switch p_{t+1} is defined in the range [0.5, 1] with the initial switch value as 0.5. The adaptive transition is given as follows [83]:

$$p_{t+1} = \begin{cases} \dfrac{1}{1 + \exp\left(-\frac{f_t^*}{f_{t-1}^*}\right)}, & \lfloor log_{10} |f_t^*| \rfloor \\ & \neq \lfloor log_{10} |f_{t-1}^*| \rfloor \\ \dfrac{1}{1 + \exp\left(-\frac{f_t^* - \theta . \left\lfloor \frac{f_t^*}{\theta} \right\rfloor}{f_{t-1}^* - \theta . \left\lfloor \frac{f_{t-1}^*}{\theta} \right\rfloor}\right)}, & \text{otherwise} \end{cases}, \tag{31}$$

where f_t^* is the finest fitness value obtained at the tth iteration, $\lfloor . \rfloor$ is the floor function, and θ is the threshold value of the adaptive scale parameter that helps in auto-recognizing the search state and is given by

$$\theta = 10^{\lfloor log_{10} |f_t^* - f_{t-1}^*| \rfloor + 1}. \tag{32}$$

In $f_t^* >>> f_{t-1}^*$, a large difference is observed in the fitness values between two iterations. Accordingly, the adaptive switch p_{t+1} attains the value of one. Therefore, the algorithm switches to the exploitation mode for next iteration. In $f_t^* <<< f_{t-1}^*$, the adaptive switch p_{t+1} will be 0.5, and the exploration mode is selected for the next iteration. A local minimum has been found for the situation $\lfloor log_{10} |f_t^*| \rfloor = \lfloor log_{10} |f_{t-1}^*| \rfloor$. The adaptive switch ratio is modified by the term $\frac{f_t^* - \theta . \left\lfloor \frac{f_t^*}{\theta} \right\rfloor}{f_{t-1}^* - \theta . \left\lfloor \frac{f_{t-1}^*}{\theta} \right\rfloor}$ to make this adaptive switch sensitive. This improvement allows the search agents to jump out of potential traps with higher probability [83].

5) CATFISH EFFECT MECHANISM

Fishermen place catfish into a sardine pond in real life to maintain the freshness of sardines. The catfish disturbs the sardines' living environment to stimulate their ability to survive. This phenomenon derives the catfish effect and was successfully incorporated into the PSO [84]. Such a mechanism is employed to avoid premature convergence by forcing the worst solutions to explore search space and possibly obtain better solutions. According to this mechanism, if the fitness value of the current best individual has not been improved in n consecutive iterations, then the 10% worst "sardine" individuals WX will be replaced by new "catfish" individuals CX. The "catfish" individuals are considered as opposition "sardine" individuals and can be calculated as follows:

$$CX_{id} = a_d + b_d - WX_{id}, \tag{33}$$

where i is the "sardine" individuals index, and WX is 10% worst "sardine" individuals.

a: MAIN PROCEDURE OF THE AFPA

The modified AFPA is developed by integrating the EOBL technique, Cauchy distribution-based global pollination phase, LNS model, dynamic switch probability, and catfish effect mechanism in the conventional FPA. The detailed pseudocode of the AFPA is shown in Algorithm 2.

Algorithm 2 : Pseudocode of AFPA-EERP

Input: Define objective function
$f(x), x = (x1, x2, \ldots, xD)$
Output: Identify current best solution X_{best}^t;
Initialization: Initialize related parameters,
Initialize the dynamic boundary of the search space,
Randomly initialize a population P of NP random flowers
while the stop criterion is not satisfied *do*
Update the current population with EOBL according to Equations (19)–(22);
while iterations < maximum number of iterations
for i = 1: NP
if rand $< p_t$
perform global pollination:
$X_i^{t+1} = X_i^t + C(\delta)(X_{best}^t - X_i^t)$
else
perform local pollination by using Equations (28) and (29)
end if
evaluate X_i^{t+1}
if X_i^{t+1} *is better than* X_i^t, *update*
end if
Update p_t *using equation (31) and (32)*
end for
Find the solution with the best fitness value.
Update X_{best}^t *if the current best solution better than the previous best solution.*
Apply catfish effect mechanism using equation (33).
Return to the next generation until stop criterion is achieved.
end while
update final best X_{best}^t
end

b: STEADY-STATE PHASE

Steady-state phase is categorized into two parts, namely, intra-zone and inter-zone data transmission phases. The interval for the transmission of the message/data in the steady-state phase is far lengthier than that in the set-up phase. Hence, the reduction of energy dissipation in the steady-state phase can be considered an appealing opportunity. Considering the intra-zone data transmission phase (being a part of the reactive protocol), the member nodes transmit information to the ZCH after a certain time interval t and perform exploration for the rest of the time. During the inter-zone data transmission phase, the ZCH receives data from other ZCHs and sends the accumulated data to the next hop. The next hop also depends on the distance between the BS and the ZCH, denoted as d_{ZCH-BS} at the time-slot, which is assigned by the upper level ZCH.

c: INTRA-ZONE DATA TRANSMISSION PHASE

The energy of active robots during this data transmission phase will be dissipated during sensing, navigation, packet transmission, receiving, and aggregation. The energy of ZCHs will also be consumed with packet reception and aggregation. Thus, the energy of the ZMRs and ZCHs in this phase can be formally modified in accordance with the following expression:

$$E\left(X_m\right) = E\left(X_m\right) - E_{sensing}(X_m) - E_{TX}(X_m, ZCH_k) \tag{34}$$

$$E\left(ZCH_k\right) = E\left(ZCH_k\right) - (E_{RX} + E_D), \tag{35}$$

where $E\left(X_m\right)$ and $E\left(ZCH_k\right)$ denote the current energy of the m^{th} ZMR and k^{th} ZCH, respectively; $E_{TX}(X_m, ZCH_k)$ is the energy expenditure for transmitting data from the ZMR to the ZCH; E_{RX} is the energy dissipated for reception of data at the ZCH; and E_D is the energy dissipated in data aggregation for ZCH.

d: INTER-ZONE DATA TRANSMISSION PHASE

During this phase, the energy of ZCHs in the network will be modified according to the dissipated energy required for packet transmission to the BS. Energy is also dissipated for relay ZCHs (i.e., ZCH_R to receive the message packets from the distant ZCHs and transmission to next ZCH). In this phase, the energy of the ZCH can be formally modified according to the following expression:

$$E\left(ZCH_k\right) = \begin{cases} E\left(ZCH_R\right) - E_{TX}(ZCH_k, ZCH_R) \\ \qquad if\ d(ZCH_k, BS) \geq V_D \\ E\left(ZCH_k\right) \\ -(E_{RX} + E_D + E_{TX}(ZCH_k, BS)) \\ \qquad if\ d(ZCH_k, BS) < V_D \end{cases}, \tag{36}$$

where $d(ZCH_k, BS)$ is the distance between the ZCH and the BS, ZCH_R is the relay ZCH that lies within the transmission/reception range V_D, and $E(ZCH_k)$ is the residual energy of ZCHs. Improving the communication efficiency and reducing the long communication cost by using A-FPA with multi-hop communication have been proposed in this routing algorithm. If the distance $d(ZCH_k, BS)$ is greater than V_D, then an adjacent ZCH must be considered as a relay to send its data to the BS. Relative distance factor (D_f) is considered to achieve load balancing, and it is defined as follows:

$$f_3 = D_f = \frac{d(ZCH_k, ZCH_R)^2 + d(ZCH_R, BS)^2}{\max\limits_{k,R}\left(d(ZCH_k, ZCH_R)^2 + d(ZCH_R, BS)^2\right)}. \tag{37}$$

Distance factor D_f is associated with the total sum of distance in-between the source ZCH and relay ZCH and relay ZCH and BS. If ZCH_k is away from the BS, then it chooses a ZCH_R as a relay node. ZCH_R with the least cost of link will be selected to relay the data sensed by ZCH_k.

VI. SIMULATION RESULTS

The design of the network scenario, which executes AFPA-EERP for ZCH selection and optimal route establishment, is demonstrated via computer-aided simulation to optimize energy consumption of robots in MRS.

The simulation results of AFPA-EERP have been analyzed in terms of performance metrics, such as energy efficiency and network lifetime, performance at different energy levels, and effect of robot density, and compared with LEACH [39], hierarchical cluster-based routing (HCR) [85], evolutionary-based clustered routing protocol (ERP) [86], distance-based residual energy efficient stable election protocol (DRESEP) [87], harmony search algorithm-based energy-efficient routing protocol (HSAERP) [88], Ant colony optimization energy efficient routing protocol (ACO-EERP) [57], and Distance Aware Residual Energy-efficient Stable Election Protocol (DARE-SEP) [89].

The mobile robots are considered to be powered by a Lithium-Polymer (Li-Po) battery (2200 mAh = 88 kJ) [90], which drives motors, control systems, and sensors. A portion of energy (330 mAh = 13 kJ) is assumed to be used for powering the LoRa module (Microchip RN2483) [69] for transmitting and receiving data. The parameters used for the protocol simulations in the network are described in Table 2.

A. ENERGY EFFICIENCY

We considered the metrics of lifetime and total consumed energy to comparatively evaluate the schemes and methods proposed by this research. The simulation results are produced by deploying 10 robots per outer zone, making a total of 80 robots. The network consists of robots having initial energy E_0, and the BS is located at (50, 120) (i.e., outside the area to be explored). The A-FPA protocol performance is evaluated in terms of stability period (the time interval or the rounds before the first robot becomes inactive due to energy depletion) and network lifetime and further compared with the other algorithms.

TABLE 2. Simulation parameters.

Parameter	Value
Number of robots	80
Simulator	MATLAB R2020a
Area	1000 m × 1000 m
Location of the BS	(50, 120) (outside area)
Length of data packet	40,000 bits
Initial energy, E_0	13, 6.66, and 2.26 kJ
Radio energy, $E_{TX} = E_{RX}$	500 $\mu J/bit$
Energy for data-aggregation, E_D	50 $\mu J/bit$
Radio amplifier energy, ε_{friis_amp}	1000 $nJ/bit/m^2$
Radio amplifier energy, $\varepsilon_{two\_ray\_amp}$	0.013 $nJ/bit/m^4$
Routing protocols	AFPA-EERP, LEACH, HCR, ERP, DRESEP, HSAERP, ACO-EERP, and DARE-SEP

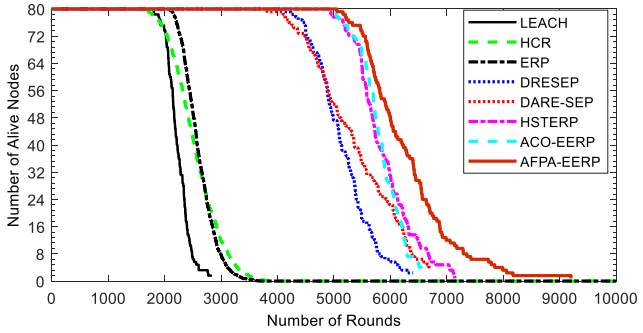

FIGURE 9. Comparison of no. of alive robots per round wrt different protocols for E0 = 13kJ.

The interval between successive reformations to the cluster is referred to as a single round. The predetermined number of clusters required for comparison by the current algorithms is set at 5%. The results are averaged over 20 random setups. The simulation results for energy efficiency are shown in Figure 9. In comparison with state-of-the-art algorithms, the AFFA-EERP utilizes ZCHs and the BS to establish the feasible routing set for each ZCH to obtain their optimal routes. This mechanism reduces the effect of randomness, which contributes to the balanced energy consumption of the ZCHs, improves energy efficiency, and reduces the computational complexity of the algorithm.

B. NETWORK LIFETIME

The network's lifetime is calculated by the number of live robots that will be evaluated at each round. The lifetime of the network and the total amount of data transferred are measured by assessing the number of rounds until the death of the last robot. A robot whose battery energy level is lower than the energy required for accurate sensing or processing is termed as a dead robot. The simulation results for the total network lifetime are shown in terms of the normalized energy for competitive protocols with initial energy

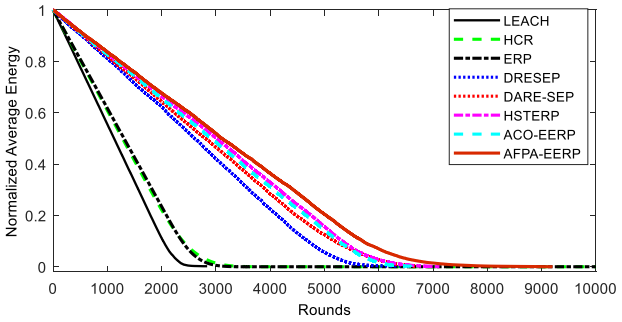

FIGURE 10. Comparison of normalized energy per round wrt different protocols for E0 = 13kJ.

E_0 = 13 kJ (Figure 10). AFPA-EERP has a maximum network lifetime because of the reason optimal selection of ZCHs and routing path by using A-FPA on the basis of energy and distance. The performance advantage of A-FPA in terms of the total network lifetime is ∼4% compared with HSAERP and ∼10% compared with DARE-SEP when 50% of the robots are alive. The performance drastically improves till the last robot is alive (i.e., ∼20% compared with HSAERP and ∼26% compared with DARE-SEP).

AFFA-EERP improves the network lifespan because it considers the remaining energy of the robots for the ZCH selection. The improvements achieved by the AFFA-EERP scheme point to the ability to balance the energy through the robots. In AFFA-EERP, the robot with the higher remaining energy, nearer to the BS, higher density, and concentration has the best chance to become the ZCH. This improved network lifetime is a result of a better selection of the ZCHs and interchanging the load over the nodes in a more balanced approach.

C. PERFORMANCE AT DIFFERENT ENERGY LEVELS

Herein, three cases are simulated at different initial energy levels for communication (i.e., $\boldsymbol{E_0}$ = 13 kJ [100%], $\boldsymbol{E_0}$ = 6.66 kJ [≈50%], and $\boldsymbol{E_0}$ = 2.26 kJ [≈25%]). The simulations are performed with different initial energy levels of the robots to verify the performance of the proposed algorithm. Tables 3, 4, and 5 show the dead robots round history for $\boldsymbol{E_0}$ = 2.26, 6.66, and 13 kJ, respectively. With regard to the total network lifetime (i.e., time until last the robot dead [LRD]) and the stability period (i.e., time until the first robot dead [FRD]), the proposed protocol outperforms against all other protocols.

D. EFFECT OF ROBOT DENSITY

To assess the effect of robot density or scalability in each approach, the robots are assumed to have an initial energy of 13 KJ. The same parameters are used to construct the simulation model as in a 100-robot scenario, and the results are shown for homogeneous setups in Table 6. The effect of robot density is evaluated in each approach by varying the number of robots from 100 to 500. A comparative evaluation of AFPA-EERP is conducted to illustrate and validate

TABLE 3. Dead robots round history for E0 = 2.26 kJ.

% dead robots	LEACH	HCR	ERP	DRESEP	DARE-SEP	HSAERP	ACO-EERP	AFPA-EERP
1 (FRD)	461.2	441.9	510.8	782.4	773.6	1224.4	1219.4	**1262.3**
10	486.6	498.4	588	1132.2	1130.4	1315.4	1317.4	**1377.8**
20	504.1	514.2	608.6	1232.5	1235.9	1372.0	1385.6	**1413.5**
30	513.5	537.4	629.1	1282.7	1306.4	1392.9	1409.3	**1450.9**
40	523	559.8	641.6	1342.7	1376.3	1418.9	1434.6	**1498.9**
50 (HRD)	568	598.4	646.9	1392.4	1416.8	1443.3	1450.3	**1552.2**
60	590.7	609.4	658.6	1421.3	1453.5	1494.6	1505.7	**1603.8**
70	590.6	619.1	674.9	1442.2	1485.4	1531.2	1542.4	**1639.1**
80	607.6	625.4	701.7	1492.3	1548.7	1575.0	1574.7	**1716.1**
90	630.9	636.1	732.5	1542.1	1624.8	1665.6	1642.8	**1820.9**
100 (LRD)	745.6	848.7	784.3	1602.2	1688.8	1776.2	1708.4	**2041.2**

TABLE 4. Dead robot round history for E0 = 6.66 kJ.

% dead robots	LEACH	HCR	ERP	DRESEP	DARE-SEP	HSAERP	ACO-EERP	AFPA-EERP
1 (FRD)	971.6	871.4	1039.1	1563.8	1538.6	2439.5	2417.5	**2514.1**
10	1006.4	1008.6	1159.5	2263.4	2242.8	2621.5	2618.3	**2745.1**
20	1038.2	1061.6	1199.7	2464.9	2461.5	2734.75	2739.4	**2819.1**
30	1061.5	1114.2	1238.6	2561.4	2571.8	2776.45	2812.7	**2893.9**
40	1074.9	1164.9	1266.9	2681.6	2695.7	2832.55	2859.5	**2985.9**
50 (HRD)	1168.6	1229.6	1293.9	2781	2863.6	2877.3	2905.2	**3094.1**
60	1207.9	1266.9	1318.8	2842.9	2915.9	2977.85	2981.5	**3198.9**
70	1266.6	1307.2	1361.1	2881.4	2974.2	3051.1	3021.7	**3267.1**
80	1317.5	1354.6	1411	2981.9	3105.4	3138.8	3103.7	**3424.2**
90	1368.2	1412.9	1478.3	3081.5	3217.6	3321.9	3289.6	**3634.1**
100 (LRD)	1671.8	1742.3	1608.8	3201.3	3389.4	3543.2	3403.6	**4074.9**

TABLE 5. Round history of dead robots for E0 = 13 kJ.

% dead robots	LEACH	HCR	ERP	DRESEP	DARE-SEP	HSAERP	ACO-EERP	AFPA-EERP
1 (FRD)	1806.2	1727	2114.3	4102.6	3892.7	4902.8	4897.4	**5053.1**
10	2021.8	2049.6	2277.3	4505.2	4474.6	5266.8	5272.7	**5516.5**
20	2068.3	2188.6	2365.4	4768.9	4729.2	5493.3	5503.7	**5666.1**
30	2142	2316.3	2439	4882.4	4890.4	5576.7	5592.3	**5811.1**
40	2168.4	2421.2	2508.5	4984.5	5045.9	5688.9	5705.7	**5997.1**
50 (HRD)	2216.2	2525.6	2581	5127.7	5284.5	5778.4	5770.2	**6209.1**
60	2281.1	2628.9	2649.9	5295.2	5407.4	5983.5	5927.6	**6423.9**
70	2347.3	2753.2	2745.8	5396.4	5657.5	6128	6104.3	**6565.1**
80	2395.8	2917.8	2838.3	5622.1	6187.5	6305.4	62.53.8	**6873.9**
90	2486.6	3108.1	2984.3	5771.7	6319.3	6667.6	6559.5	**7292.1**
100 (LRD)	2764.5	3575.3	3306.9	6403.2	6764.7	7108.2	6784.4	**9272.7**

its behavior under various densities (i.e., sparse, moderate, or dense). The performance of AFPA-EERP confirms that the consistency, firmness, and scalability of the proposed algorithm are great and is appropriate to large-scale MRS communication in exploration tasks.

The performance improvement of the proposed AFPA-EERP over competitive algorithms is with the increase in the network size. The proposed method seeks a solution that is more energy-efficient than others by finding the efficient energy consumption model for CHRs.

TABLE 6. Effect of robot density on the performance of AFPA-EERP.

Protocol	100	200	300	400	500
LEACH	2764.5	3038.9	3317.5	3593.6	3849.1
HCR	3575.4	4004.1	4218.8	4433.4	4683.3
ERP	3306.8	3571.5	3714.4	3825.7	4016.8
DRESEP	6403.2	7491.7	8015.6	8977.3	10144.7
DARE-SEP	6764.7	7538.5	8063.9	9052.6	10185.4
HSAERP	7108.2	7821.1	8446.7	9091.75	10228.5
ACO-EERP	6784.4	7659.6	8269.4	8810.8	9963.9
AFPA-EERP	**9272.7**	**9547.1**	**9846.9**	**10747.9**	**12247.5**

VII. CONCLUSION AND FUTURE SCOPE

In this correspondence, various approaches for multi-robot communication were reviewed, considering the communication constraints involved in the field of multi-robot communication. This work addresses the problem of routing of data by robots, which are spatially dispersed in zones, to the BS at specific time instants while ensuring an efficient communication and increased network life time. A framework for multi-robot communication by using AFPA-EERP is proposed for transmission and routing of data between ZMR and ZCH, ZCH and ZCH, and ZCH and BS. This information is further utilized by the SLAM protocol at the BS for efficient exploration and map making. Periodic communication helps the BS in generating updated poses for ZMRs to empower the exploration, which in turn saves robot's energy. The simulation results show that the proposed protocol (i.e., AFPA-EERP) can be effectively applied in the MRS for unknown outdoor environment exploration because it outperforms other methods (available in literature) in terms of energy efficiency and network life time.

In the future, the investigation and applicability of the proposed protocol on hardware for communication in outdoor map making applications will be explored. The formation of the robots will be different in the case of indoor environments; hence, further modifications of the algorithm will be required to suit it for indoor applications. Finally, this development will also incorporate open-source codes and hardware schematics to empower researchers around the globe to develop applications for MRS. Analyzing the trust level of a robot is also an important aspect of the MRS, using which two robots can communicate with trust because an untrustworthy robot has an adverse effect on the quality and reliability of the data.

REFERENCES

[1] A. Farinelli, L. Iocchi, and D. Nardi, "Multirobot systems: A classification focused on coordination," *IEEE Trans. Syst., Man Cybern. B, Cybern.*, vol. 34, no. 5, pp. 2015–2028, Oct. 2004.

[2] H. Ding, E. Cristofalo, J. Wang, D. Castanon, E. Montijano, V. Saligrama, and M. Schwager, "A multi-resolution approach for discovery and 3-D modeling of archaeological sites using satellite imagery and a UAV-borne camera," in *Proc. Amer. Control Conf. (ACC)*, Jul. 2016, pp. 1359–1365.

[3] E. Montijano, E. Cristofalo, D. Zhou, M. Schwager, and C. Sagues, "Vision-based distributed formation control without an external positioning system," *IEEE Trans. Robot.*, vol. 32, no. 2, pp. 339–351, Apr. 2016.

[4] Z. Wang and M. Schwager, "Multi-robot manipulation without communication," in *Distributed Autonomous Robotic Systems*. Boulder, CO, USA: Springer, 2016, pp. 135–149.

[5] P. Culbertson and M. Schwager, "Decentralized adaptive control for collaborative manipulation," in *Proc. IEEE Int. Conf. Robot. Autom. (ICRA)*, May 2018, pp. 278–285.

[6] N. Usevitch, Z. Hammond, S. Follmer, and M. Schwager, "Linear actuator robots: Differential kinematics, controllability, and algorithms for locomotion and shape morphing," in *Proc. IEEE/RSJ Int. Conf. Intell. Robots Syst. (IROS)*, Sep. 2017, pp. 5361–5367.

[7] A. Khamis. (2016). *Cooperative Multi-robot Systems*. Accessed: Sep. 13, 2020. [Online]. Available: https://docplayer.net/62063522-Cooperative-multi-robot-systems.html

[8] L. Iocchi, D. Nardi, and M. Salerno, "Reactivity and deliberation: A survey on multi-robot systems," in *Proc. Workshop Balancing Reactivity Social Deliberation Multi-Agent Syst.*, 2000, pp. 9–32.

[9] D. Pickem, *Self-Reconfigurable Multi-Robot Systems*. Atlanta, Georgia: Georgia Institute of Technology, 2016.

[10] Z. Yan, L. Fabresse, J. Laval, and N. Bouraqadi, "Team size optimization for multi-robot exploration," in *Int. Conf. Simul., Model., Program. Auto. Robots*, 2014, pp. 438–449.

[11] S. Verret and D. Suffield, "Current state of the art in multirobot systems," DRDC Suffield, Medicine Hat, AB, Canada, Tech. Memo. TM 2005-241, Dec. 2005.

[12] E. Pagello, A. D'Angelo, and E. Menegatti, "Cooperation issues and distributed sensing for multirobot systems," *Proc. IEEE*, vol. 94, no. 7, pp. 1370–1383, Jul. 2006.

[13] M. J. Spenko, G. C. Haynes, J. A. Saunders, M. R. Cutkosky, A. A. Rizzi, R. J. Full, and D. E. Koditschek, "Biologically inspired climbing with a hexapedal robot," *J. Field Robot.*, vol. 25, nos. 4–5, pp. 223–242, 2008.

[14] A. Nayyar, N. G. Nguyen, R. Kumari, and S. Kumar, "Robot path planning using modified artificial bee colony algorithm," in *Frontiers in Intelligent Computing: Theory and Applications*. Da Nang, Vietnam: Duy Tan Univ., 2020, pp. 25–36.

[15] B. MacLennan, "Synthetic ethology: An approach to the study of communication," Comput. Sci. Dept. Knoxville, Univ. Tennessee, Knoxville, TN, USA, Tech. Rep. 37996-1301, 1990.

[16] R. Doriya, S. Mishra, and S. Gupta, "A brief survey and analysis of multi-robot communication and coordination," in *Proc. Int. Conf. Comput., Commun. Autom.*, May 2015, pp. 1014–1021.

[17] I. F. Akyildiz, W. Su, Y. Sankarasubramaniam, and E. Cayirci, "A survey on sensor networks," *IEEE Commun. Mag.*, vol. 40, no. 8, pp. 102–114, Aug. 2002.

[18] E. Casarini and M. Martinelli, "Updating communication maps for exploring multirobot systems," M.S. thesis, Univ. Milan, Milano, Italy, 2017.

[19] M. O. F. Sarker, T. S. Dahl, and T. Yasuda, "Bio-inspired communication for self-regulated multi-robot systems," in *Multi-Robot Systems, Trends and Development*. London, U.K.: InTech, 2011, pp. 367–392.

[20] J. Banfi, A. Q. Li, I. Rekleitis, F. Amigoni, and N. Basilico, "Strategies for coordinated multirobot exploration with recurrent connectivity constraints," *Auto. Robots*, vol. 42, no. 4, pp. 875–894, Apr. 2018.

[21] J. C. G. Reis, P. U. Lima, and J. Garcia, "Efficient distributed communications for multi-robot systems," in *Robot Soccer World Cup*. Berlin, Germany: Springer, 2013, pp. 280–291.

[22] A. Speranzon, *On Control Under Communicaiton Constraints in Autonomous Multi-Robot Systems*. Stockholm, Sweden: Signaler, Sensorer Och System, 2004.

[23] I. F. Akyildiz, T. Melodia, and K. R. Chowdhury, "A survey on wireless multimedia sensor networks," *Comput. Netw.*, vol. 51, no. 4, pp. 921–960, Mar. 2007.
[24] I. U. Khan, I. M. Qureshi, M. A. Aziz, T. A. Cheema, and S. B. H. Shah, "Smart IoT control-based nature inspired energy efficient routing protocol for flying ad hoc network (FANET)," *IEEE Access*, vol. 8, pp. 56371–56378, 2020.
[25] I.-A. Gal, L. Vladareanu, R. I. Munteanu, A. Ciocîrlan, and A.-M. Travediu, "Smart wireless sensors routing protocol development aimed for smart wireless robot networks," *Acta Electroteh.*, vol. 61, pp. 1–7, Jan. 2020.
[26] M. H. Hassan, S. A. Mostafa, H. Mahdin, A. Mustapha, A. A. Ramli, M. H. Hassan, and M. A. Jubair, "Mobile ad-hoc network routing protocols of time-critical events for search and rescue missions," *Bull. Electr. Eng. Informat.*, vol. 10, no. 1, pp. 192–199, Feb. 2021.
[27] A. Dutta, A. Ghosh, S. Sisley, and O. P. Kreidl, "Efficient communication in large multi-robot networks," in *Proc. IEEE Int. Conf. Robot. Autom. (ICRA)*, May 2020, pp. 6647–6653.
[28] F. Hu and X. Cao, *Wireless Sensor Networks: Principles and Practice*. Boca Raton, FL, USA: CRC Press, 2010.
[29] L. Ding, B. Han, X. Wang, P. Li, and B. Wang, "Distributed intelligence empowered data aggregation and distribution for multi-robot cooperative communication," in *Proc. IEEE INFOCOM Conf. Comput. Commun. Workshops (INFOCOM WKSHPS)*, Jul. 2020, pp. 622–627, doi: 10.1109/INFOCOMWKSHPS50562.2020.9162700.
[30] K.-C. Chen, S.-C. Lin, J.-H. Hsiao, C.-H. Liu, A. F. Molisch, and G. P. Fettweis, "Wireless networked multirobot systems in smart factories," *Proc. IEEE*, vol. 109, no. 4, pp. 468–494, Apr. 2021.
[31] J. Gregory, J. Fink, E. Stump, J. Twigg, J. Rogers, D. Baran, N. Fung, and S. Young, "Application of multi-robot systems to disaster-relief scenarios with limited communication," in *Field and Service Robotics*. Cham, Switzerland: Springer, 2016, pp. 639–653.
[32] Y. Cheriguene, S. Djellikh, F. Z. Bousbaa, N. Lagraa, A. Lakas, C. A. Kerrache, and A. E. K. Tahari, "SEMRP: An energy-efficient multicast routing protocol for UAV swarms," in *Proc. IEEE/ACM 24th Int. Symp. Distrib. Simulation Real Time Appl. (DS-RT)*, Sep. 2020, pp. 1–8.
[33] H. Xiao, Z. Hu, K. Yang, Y. Du, and D. Chen, "An energy-aware joint routing and task allocation algorithm in MEC systems assisted by multiple UAVs," in *Proc. Int. Wireless Commun. Mobile Comput. (IWCMC)*, Jun. 2020, pp. 1654–1659.
[34] Z. Jin and X. Zeng, "Research on a multi-robot routing optimization method based on hybrid Lora location," in *Proc. 5th Int. Conf. Control, Robot. Cybern. (CRC)*, Oct. 2020, pp. 221–225.
[35] N. A. Pantazis, S. A. Nikolidakis, and D. D. Vergados, "Energy-efficient routing protocols in wireless sensor networks: A survey," *IEEE Commun. Surveys Tuts.*, vol. 15, no. 2, pp. 551–591, 2nd Quart., 2013.
[36] J. Reich and E. Sklar, "Robot-sensor networks for search and rescue," in *Proc. IEEE Int. Workshop Saf., Secur. Rescue Robotics*, vol. 22, Aug. 2006, pp. 1–6.
[37] N. Sadagopan, B. Krishnamachari, and A. Helmy, "Active query forwarding in sensor networks," *Ad Hoc Netw.*, vol. 3, no. 1, pp. 91–113, Jan. 2005.
[38] W. R. Heinzelman, J. Kulik, and H. Balakrishnan, "Adaptive protocols for information dissemination in wireless sensor networks," in *Proc. 5th Annu. ACM/IEEE Int. Conf. Mobile Comput. Netw. (MobiCom)*, Aug. 1999, pp. 174–185.
[39] S. Deng, L. Shen, and J. Li, "Mobility-based clustering protocol for wireless sensor networks with mobile nodes," *IET Wireless Sensor Syst.*, vol. 1, no. 1, pp. 39–47, Mar. 2011.
[40] W. B. Heinzelman, A. P. Chandrakasan, and H. Balakrishnan, "An application-specific protocol architecture for wireless microsensor networks," *IEEE Trans. Wireless Commun.*, vol. 1, no. 4, pp. 660–670, Oct. 2002.
[41] S. Lindsey and C. S. Raghavendra, "PEGASIS: Power-efficient gathering in sensor information systems," in *Proc. IEEE Proc. Aerosp. Conf.*, Mar. 2002, p. 3.
[42] A. Manjeshwar and D. P. Agrawal, "TEEN: A routing protocol for enhanced efficiency in wireless sensor networks," in *Proc. 15th Int. Parallel Distrib. Process. Symp. (IPDPS)*, Apr. 2001, pp. 304–309.
[43] A. Manjeshwar and D. P. Agrawal, "APTEEN: A hybrid protocol for efficient routing and comprehensive information retrieval in wireless," in *Proc. 16th Int. Parallel Distrib. Process. Symp.*, 2002, p. 0195.
[44] S. Basagni, I. Chlamtac, V. R. Syrotiuk, and B. A. Woodward, "A distance routing effect algorithm for mobility (DREAM)," in *Proc. 4th Annu. ACM/IEEE Int. Conf. Mobile Comput. Netw. (MobiCom)*, Oct. 1998, pp. 76–84.
[45] Y. Yu, R. Govindan, and D. Estrin, "Geographical and energy aware routing: A recursive data dissemination protocol for wireless sensor networks," UCLA, Los Angeles, CA, USA, Tech. Rep. UCLA/CSD-TR-01-0023, 2001.
[46] S. Son, B. Blum, T. He, and J. Stankovic, "IGF: A state-free robust communication protocol for wireless sensor networks," Dept. Comput. Sci. Univ. Virginia, Charlottesville, VA, USA, Tech. Rep. CS-2003-11, 2003.
[47] D. Chen and P. K. Varshney, "On-demand geographic forwarding for data delivery in wireless sensor networks," *Comput. Commun.*, vol. 30, nos. 14–15, pp. 2954–2967, Oct. 2007.
[48] M. Chen, V. C. M. Leung, S. Mao, Y. Xiao, and I. Chlamtac, "Hybrid geographic routing for flexible energy—Delay tradeoff," *IEEE Trans. Veh. Technol.*, vol. 58, no. 9, pp. 4976–4988, Nov. 2009.
[49] K. Sohrabi, J. Gao, V. Ailawadhi, and G. J. Pottie, "Protocols for self-organization of a wireless sensor network," *IEEE Pers. Commun.*, vol. 7, no. 5, pp. 16–27, Oct. 2000.
[50] T. He, J. A. Stankovic, C. Lu, and T. Abdelzaher, "SPEED: A stateless protocol for real-time communication in sensor networks," in *Proc. 23rd Int. Conf. Distrib. Comput. Syst.*, May 2003, pp. 46–55.
[51] E. Felemban, C.-G. Lee, and E. Ekici, "MMSPEED: Multipath multi-SPEED protocol for QoS guarantee of reliability and. Timeliness in wireless sensor networks," *IEEE Trans. Mobile Comput.*, vol. 5, no. 6, pp. 738–754, Jun. 2006.
[52] M. Chen, C.-F. Lai, and H. Wang, "Mobile multimedia sensor networks: Architecture and routing," *EURASIP J. Wireless Commun. Netw.*, vol. 2011, no. 1, p. 159, Dec. 2011.
[53] A. Nayyar and N. G. Nguyen, "Introduction to swarm intelligence," in *Advances in Swarm Intelligence for Optimizing Problems in Computer Science*. London, U.K.: Chapman & Hall, 2018, pp. 53–78.
[54] A. Nayyar, D.-N. Le, and N. G. Nguyen, *Advances in Swarm Intelligence for Optimizing Problems in Computer Science*. Boca Raton, FL, USA: CRC Press, 2018.
[55] K. Deb, A. Pratap, S. Agarwal, and T. Meyarivan, "A fast and elitist multiobjective genetic algorithm: NSGA-II," *IEEE Trans. Evol. Comput.*, vol. 6, no. 2, pp. 182–197, Apr. 2002.
[56] I. C. Trelea, "The particle swarm optimization algorithm: Convergence analysis and parameter selection," *Inf. Process. Lett.*, vol. 85, no. 6, pp. 317–325, Mar. 2003.
[57] M. Dorigo and G. Di Caro, "Ant colony optimization: A new meta-heuristic," in *Proc. Congr. Evol. Comput. (CEC)*, Jul. 1999, pp. 1470–1477.
[58] Z. W. Geem, J. H. Kim, and G. V. Loganathan, "A new heuristic optimization algorithm: Harmony search," *Simulation*, vol. 76, no. 2, pp. 60–68, Feb. 2001.
[59] X.-S. Yang, M. Karamanoglu, and X. He, "Flower pollination algorithm: A novel approach for multiobjective optimization," *Eng. Optim.*, vol. 46, no. 9, pp. 1222–1237, Sep. 2014.
[60] X.-S. Yang, "Flower pollination algorithm for global optimization," in *Proc. Int. Conf. Unconventional Comput. Natural Comput.*, 2012, pp. 240–249.
[61] N. Mittal, "Moth flame optimization based energy efficient stable clustered routing approach for wireless sensor networks," *Wireless Pers. Commun.*, vol. 104, no. 2, pp. 677–694, Jan. 2019.
[62] P. Saxena and A. Kothari, "Linear antenna array optimization using flower pollination algorithm," *SpringerPlus*, vol. 5, no. 1, p. 306, Dec. 2016.
[63] L. Murata Manufacturing Co. (2017). *MA40S4S/MA40S4R Ultrasonic Sensor. Resource Document*. Accessed Sep. 23, 2020. [Online]. Available https://www.murata.com/~/media/webrenewal/products/sensor/ultrasonic/open/datasheet_maopn.ashx?la=en
[64] D. Instruments. (2010). *AR1000 Laser Distance Sensor. Resource Document*. Accessed: Sep. 23, 2020. [Online]. Available: http://www.disensors.com/downloads/products/AR1000LaserDistanceSensor_1080.pdf
[65] O. Corporation. (2012). *D6T-44L / -8L / -1A Thermal Sensor*. Accessed: Sep. 23, 2020. [Online]. Available: https://www.components.omron.com/documents/35730/96733/AN-D6T-01EN_r2.pdf/fb9c9fdd-4d2a-df6a-77b9-234c07be20a8
[66] STMicroelectronics. (2015). *VB6955CMQ0GH/1 5.0 Megapixel Auto-Focus Camera Module. Resource Document*. Accessed: Sep. 23, 2020. [Online]. Available http://www.st.com/content/ccc/resource/technical/document/datasheet/0c/98/8c/81/74/ff/41/73/DM00240130.pdf/files/DM00240130.pdf/jcr:content/translations/en.DM00240130.pdf

[67] L. Technology. (2006). *LS20030-3 GPS Smart Antenna Module*. Accessed: Sep. 23, 2020. [Online]. Available: https://www.sparkfun.com/datasheets/GPS/Modules/LS20030~3_datasheet_v1.0.pdf

[68] T. Instruments. (2011). *CC1120 High-Performance RF Transceiver*. Accessed: Sep. 23, 2020. [Online]. Available: http://www.ti.com/lit/ds/symlink/cc1120.pdf

[69] Microchip. (2015). *RN2483 Low-Power Long Range LoRa*. Accessed: Sep. 23, 2020. [Online]. Available: http://ww1.microchip.com/downloads/en/DeviceDoc/50002346C.pdf

[70] S. Corporation. (2017). *SX1272/73. Low Power Long Range Transceiver. Wireless & Sensing Products*. Accessed: Sep. 23, 2020. [Online]. Available: https://www.semtech.com/uploads/documents/sx1272.pdf

[71] S. Hening, C. A. Ippolito, K. S. Krishnakumar, V. Stepanyan, and M. Teodorescu, "3D LiDAR SLAM integration with GPS/INS for UAVs in urban GPS-degraded environments," in *Proc. AIAA Inf. Syst.-AIAA Infotech @ Aerosp.*, Jan. 2017, p. 448.

[72] M. Eck, *Simultaneous 2D Localization and 3D Mapping on a Mobile Robot With Time-of-Flight Sensors*. Koblenz, Germany: Univ. Applied Sciences Koblenz, 2013.

[73] J. Aulinas, Y. R. Petillot, J. Salvi, and X. Lladó, "The slam problem: A survey," *CCIA*, vol. 184, no. 1, pp. 363–371, 2008.

[74] A. R. Vidal, H. Rebecq, T. Horstschaefer, and D. Scaramuzza, "Ultimate SLAM? Combining events, images, and IMU for robust visual SLAM in HDR and high-speed scenarios," *IEEE Robot. Autom. Lett.*, vol. 3, no. 2, pp. 994–1001, Apr. 2018.

[75] G. Grisetti, R. Kummerle, C. Stachniss, and W. Burgard, "A tutorial on graph-based SLAM," *IEEE Intell. Transp. Syst. Mag.*, vol. 2, no. 4, pp. 31–43, winter 010.

[76] A. Wallar, E. Plaku, and D. A. Sofge, "Reactive motion planning for unmanned aerial surveillance of risk-sensitive areas," *IEEE Trans. Autom. Sci. Eng.*, vol. 12, no. 3, pp. 969–980, Jul. 2015.

[77] P. Singh and N. Mittal, "An efficient localization approach to locate sensor nodes in 3D wireless sensor networks using adaptive flower pollination algorithm," *Wireless Netw.*, vol. 27, no. 3, pp. 1999–2014, Apr. 2021.

[78] A. Mishra and S. Deb, "Mobile robot path planning using a flower pollination algorithm-based approach," in *Nature-Inspired Computation in Navigation and Routing Problems*. Singapore: Springer, 2020, pp. 127–147.

[79] D. Rodrigues, G. H. de Rosa, L. A. Passos, and J. P. Papa, "Adaptive improved flower pollination algorithm for global optimization," in *Nature-Inspired Computation in Data Mining and Machine Learning*. Cham, Switzerland: Springer, 2020, pp. 1–21.

[80] X. Wu, Y. Zhou, and Y. Lu, "Elite opposition-based water wave optimization algorithm for global optimization," *Math. Problems Eng.*, vol. 2017, pp. 1–25, Jan. 2017.

[81] U. Singh and R. Salgotra, "Pattern synthesis of linear antenna arrays using enhanced flower pollination algorithm," *Int. J. Antennas Propag.*, vol. 2017, pp. 1–11, Feb. 2017.

[82] S. Das, A. Abraham, U. K. Chakraborty, and A. Konar, "Differential evolution using a neighborhood-based mutation operator," *IEEE Trans. Evol. Comput.*, vol. 13, no. 3, pp. 526–553, Jun. 2009.

[83] J. Wu, Y.-G. Wang, K. Burrage, Y.-C. Tian, B. Lawson, and Z. Ding, "An improved firefly algorithm for global continuous optimization problems," *Expert Syst. Appl.*, vol. 149, Jul. 2020, Art. no. 113340.

[84] L.-Y. Chuang, S.-W. Tsai, and C.-H. Yang, "Chaotic catfish particle swarm optimization for solving global numerical optimization problems," *Appl. Math. Comput.*, vol. 217, no. 16, pp. 6900–6916, Apr. 2011.

[85] S. Hussain and A. W. Matin, "Hierarchical cluster-based routing in wireless sensor networks," Acadia Univ., Wolfville, NS, Canada, Tech. Rep. TR-2005-11, 2006.

[86] E. A. Khalil and B. A. Attea, "Stable-aware evolutionary routing protocol for wireless sensor networks," *Wireless Pers. Commun.*, vol. 69, no. 4, pp. 1799–1817, Apr. 2013.

[87] N. Mittal and U. Singh, "Distance-based residual energy-efficient stable election protocol for WSNs," *Arabian J. Sci. Eng.*, vol. 40, no. 6, pp. 1637–1646, Jun. 2015.

[88] D. C. Hoang, P. Yadav, R. Kumar, and S. K. Panda, "Real-time implementation of a harmony search algorithm-based clustering protocol for energy-efficient wireless sensor networks," *IEEE Trans. Ind. Informat.*, vol. 10, no. 1, pp. 774–783, Feb. 2014.

[89] A. Naeem, A. R. Javed, M. Rizwan, S. Abbas, J. C.-W. Lin, and T. R. Gadekallu, "DARE-SEP: A hybrid approach of distance aware residual energy-efficient SEP for WSN," *IEEE Trans. Green Commun. Netw.*, vol. 5, no. 2, pp. 611–621, Jun. 2021.

[90] 4-Max. (2006). *2200mAh 3S1P 11.1V Li-Po*. Accessed: Sep. 23, 2020. [Online]. Available: https://www.4-max.co.uk/pdf/WhatthenumbersmeanwithregardstoLiPocells.pdf

KIRAN JOT SINGH (Member, IEEE) received the bachelor's and master's degrees from Punjab Technical University, the PGDM from IIM Rohtak, and the Ph.D. degree from Chandigarh University. His area of research during his Ph.D. work was human–robot interaction. He has a keen interest in embedded systems and robotics. He has filed 12 patents in Indian patent office and working on various funded projects.

ANAND NAYYAR received the Ph.D. degree in computer science in the area of wireless sensor networks and swarm intelligence from Desh Bhagat University, in 2017. He is currently working with the Graduate School, Duy Tan University, Da Nang, Vietnam. He is a Certified Professional with more than 75 professional certificates from CISCO, Microsoft, Oracle, Google, Beingcert, EXIN, GAQM, and Cyberoam. He has published more than 450 research articles in various national and international conferences and international journals (Scopus/SCI/SCIE/SSCI Indexed) with High Impact Factor. He has authored/coauthored cum edited more than 30 books of computer science. He has associated with more than 500 international conferences as a programme committee/chair/advisory board/review board member. He has five Australian Patents to his credit in the area of wireless communications, artificial intelligence, the IoT, and image processing. He is also working in the area of wireless sensor networks, the IoT, swarm intelligence, cloud computing, artificial intelligence, blockchain, cyber security, network simulation, and wireless communications. He is a member of more than 50 associations as a senior and a life member and also acts as an ACM Distinguished Speaker. He has more than 30 awards for Teaching and Research—Young Scientist, Best Scientist, Young Researcher Award, Outstanding Researcher Award, Excellence in Teaching, and many more. He is an Associate Editor of *Wireless Networks* (Springer), *IET Quantum Communications*, *IET Wireless Sensor Systems*, *IET Networks*, *IJDST*, *IJISP*, and *IJCINI*. He is also the Editor-in-Chief of IGI-Global, USA Journal titled "*International Journal of Smart Vehicles and Smart Transportation (IJSVST).*"

DIVNEET SINGH KAPOOR (Member, IEEE) received the B.E. and M.E. degrees in electronics and communication engineering from Thapar University, Patiala, in 2009 and 2011, respectively. He is currently working as an Assistant Professor with Chandigarh University. He has published articles in various national and international journals, including peer-reviewed and impact factor journals. He has also filed more than 12 patents in the Indian Patent Office. His current research interests include the Internet of Things, embedded systems, robotics, and signal processing.

NITIN MITTAL received the B.Tech. and M.Tech. degrees in electronics and communication engineering (ECE) from Kurukshetra University, Kurukshetra, India, in 2006 and 2009, respectively, and the Ph.D. degree in ECE from Chandigarh University, Mohali, India, in 2017. He is currently working as an Associate Professor with the ECE Department, Chandigarh University. His research interests include wireless sensor networks, image segmentation, and soft computing.

SHUBHAM MAHAJAN (Member, IEEE) received the B.Tech. degree from the Department of Electronics and Communication Engineering, Baba Ghulam Shah Badshah University, and the M.Tech. degree from the Department of Electronics and Communication Engineering, Chandigarh University. He is currently pursuing the Ph.D. degree with Shri Mata Vaishno Devi University (SMVDU), Katra, India. His main research interests include study of wireless communication, optical fiber losses, SS-WDM, FSO, radio over fiber and image processing, multimedia data processing, data mining, and machine learning.

AMIT KANT PANDIT (Senior Member, IEEE) is currently working as an Associate Professor and an Ex-HOD of the Department of ECE, Shri Mata Vaishno Devi University (SMVDU), Katra, India. He is a MIR Labs Member. He has 19 years of academic experience.

MEHEDI MASUD (Senior Member, IEEE) received the Ph.D. degree in computer science from the University of Ottawa, Canada. He is currently a Professor with the Department of Computer Science, Taif University, Taif, Saudi Arabia. He has authored or coauthored approximately 50 publications and refereed IEEE/ACM/Springer/Elsevier journals, conference papers, books, and book chapters. His research interests include cloud computing, distributed algorithms, data security, data interoperability, formal methods, and cloud and multimedia for healthcare. He is a member of ACM. He has served as a technical program committee member in different international conferences. He was a recipient of a number of awards, including the Research in Excellence Award from Taif University. He is on the Associate Editorial Board of IEEE Access and *International Journal of Knowledge Society Research* and the Editorial Board Member of *Journal of Software*. He also served as a Guest Editor for *Computer Science and Information Systems* journal and *Journal of Universal Computer Science*.